



Universidad Autónoma
de Madrid

Biblos-e Archivo
Repositorio Institucional UAM

Repositorio Institucional de la Universidad Autónoma de Madrid

<https://repositorio.uam.es>

Esta es la **versión de autor** del artículo publicado en:
This is an **author produced version** of a paper published in:

Journal of Physics Condensed Matter 34.27 (2022): 275701

DOI: <https://doi.org/10.1088/1361-648X/ac6720>

Copyright: © 2022 IOP Publishing Ltd

El acceso a la versión del editor puede requerir la suscripción del recurso
Access to the published version may require subscription

Analytical theory for the crossover from retarded to non-retarded interactions between metal plates

Juan Luengo-Márquez*

*Department of Theoretical Condensed Matter Physics and Instituto Nicolás Cabrera,
Universidad Autónoma de Madrid, 28049 Madrid (Spain)*

Luis G. MacDowell†

*Departamento de Química Física, Facultad de Ciencias Químicas,
Universidad Complutense de Madrid, 28040, Madrid, Spain.*

(Dated: May 12, 2022)

The van der Waals force established between two surfaces plays a central role in many phenomena, such as adhesion or friction. However, the dependence of these forces on the distance of separation between plates is very complex. Two widely different non-retarded and retarded regimes are well known, but these have been traditionally studied separately. Much less is known about the important experimentally accessible cross-over regime. In this study, we provide analytical approximations for the van der Waals forces between two plates that interpolates exactly between the short distance and long distance behavior, and provides new insight into the crossover from London to Casimir forces at finite temperature. At short distance, where the behavior is dominated by non-retarded interactions, we work out a very accurate simplified approximation for the Hamaker constant which adopts analytical form for both the Drude and Lorentz models of dielectric response. We apply our analytical expressions for the study of forces between metallic plates, and observe very good agreement with exact results from numerical calculations. Our results show that contributions of interband transitions remain important in the experimentally accessible regime of decades nm for several metals, including gold.

I. INTRODUCTION

Dispersion forces arise between any two polarizable media, and are therefore ubiquitous in nature. Even if their strength is often relatively weak at short range¹, they appear to have a significant contribution to the explanation of a wide range of phenomena²⁻⁴, such as ice premelting^{5,6}, the stabilization of thin lipid films⁷, or the adhesion of Geckos to vertical surfaces⁸.

The characterization of interactions between macroscopic bodies is often described as the result of the summation over all individual interactions between pairs of particles^{2,9-11}. For the interaction between two plates across vacuum, this view results in an energy function, $g(h)$, that decreases as the squared inverse distance of separation between the plates, h :

$$g(h) = -\frac{A_{ham}(0)}{12\pi h^2} \quad (1)$$

The Hamaker constant, $A_{ham}(0)$ is a fundamental property of the interacting bodies that lumps the magnitude of the force established between pairs of molecules. From this perspective, it is a mean field parameter that is dictated by properties of pairs of interacting particles within two macroscopic objects.

Alternatively, the more modern Lifshitz theory of the van der Waals forces^{12,13} computes the Hamaker constant considering instead the energies assigned to the electromagnetic modes of vibration allowed inside the system. The dispersion forces emerge in this approach from simultaneous fluctuations of the particles as a response to these electromagnetic waves. In this framework, $A_{ham}(0)$

is dictated instead by the collective dielectric response of the materials.

However, when the distance of separation takes large values, the picture is much more complex. As h increases, the electromagnetic waves require significant amounts of time to promote fluctuations between material patches. This happens due to the fact that the speed of light at which the electromagnetic waves move is finite, so that when the vibration frequency of the polarizable particles is large, the time of the wave to travel from atom to atom might be comparable to the period assigned to the fluctuations. This phenomenon is called retardation³, and effectively weakens the dispersive interactions for large distances.

The retardation effect is considered also in the Lifshitz theory of van der Waals forces^{12,13}. When taken into account, the Hamaker coefficients of Eq. 1 becomes a function of the distance of separation, $A_{ham} = A_{ham}(h)$. For distances close to zero, $A_{ham}(h \rightarrow 0)$ reaches a constant value expected in the absence of retardation, the Hamaker constant $A_{ham}(0)$. This short-distances regime is dubbed London regime, i.e., we talk about London dispersion forces.

On the other hand, as the distance of separation between the plates increases, $A_{ham}(h)$ decays gradually and develops a distinct h dependence, which cannot be described in terms of pairwise summation of dispersion interactions. Particularly, for two perfect metal plates in vacuum at large separation and zero temperature, Casimir showed that the energy of interaction adopts the

celebrated form¹⁴:

$$g(h) = -\frac{\pi^2 c \hbar}{720 h^3} \quad (2)$$

This result explicitly points to the non-trivial dependence of the 'Hamaker constant', which, more accurately corresponds to a Hamaker function $A(h)$ decaying as $1/h$ in this limit^{15–21}.

As a matter of fact, the interest of this result goes well beyond the mere study of surface interactions, as it conveys invaluable information on the nontrivial structure of the quantum vacuum and the role of zero-point energy in physics^{22,23}. For this reason, there has been considerable interest in verifying this prediction experimentally^{24–29}. In practice, however, it must be recognized that Eq.2 is an asymptotic result which can only be realized at zero temperature, for perfect metals. Verification of the underlying physics of Eq.2 needs to take into account the simultaneous effect of finite temperature and finite conductivity of metals^{30,31}. Nevertheless, attempts to single out asymptotic corrections to the more general result of Lifshitz and collaborators^{12,13} is difficult, and remains still a matter of discussion^{18,22,30–40}.

Recently, a promising approach for the study of the crossover regime from retarded to non-retarded interactions was proposed^{41,42}. The result provided well known exact analytic results over the full range of plate separations, albeit within the so called dipole approximation of the Lifshitz equation. The key idea in that study is a quadrature rule which allows to describe the crossover regime in a non-perturbative manner. This is a significant issue, because in the Lifshitz result, plate separation, temperature and dielectric properties are entangled in a highly non-trivial manner, so it is not clear whether each effect can be singled out separately.

In this study, we aim to extend that work beyond the linear dipole approximation, which is required in order to obtain the exact Casimir limit for perfect metals at zero temperature.

In the next section we provide the essential background to the Lifshitz theory of intermolecular forces. In section III we extend the recently introduced Weighted Quadrature Approximation (WQA) beyond the dipole approximation. The working formulae relies on knowledge of the exact Hamaker constant at zero plate separation. Therefore, we devote section IV to derive a new, simple and accurate approximation for the Hamaker constant $A_{ham}(0)$. In the next section, we work out analytical results for retarded interactions between materials obeying the Drude model of the dielectric responses. In Section VI we compare the resulting interaction coefficients with exact numerical solutions of Lifshitz theory calculated from a detailed description of dielectric properties published recently^{43,44}, showing how the new methodology for the computation of the Hamaker constant proposed in this article yields values of $A_{ham}(0)$ in excellent agreement with the ones predicted by the exact Lifshitz formula. Our results are summarized in the Conclusions.

II. LIFSHITZ THEORY

In the frame of Lifshitz theory, the Hamaker function for retarded interactions between two metal plates across vacuum takes the form⁴⁵

$$A_{ham}(h) = \frac{3k_B T}{2} \sum_{n=0}^{\infty} \int_{r_n}^{\infty} \sum_{k=1}^{\infty} x dx \frac{(\Delta_{mv}^E)^{2k} + (\Delta_{mv}^M)^{2k}}{k} e^{-kx} \quad (3)$$

Where $r_n = 2h\epsilon_v^{1/2}\omega_n/c$, k_B is the Boltzmann's constant and T is the temperature in Kelvin. All along this study we employ room temperature, $T = 300$ K. Besides, we have that

$$\Delta_{mv}^E = \frac{x_v - x_m}{x_v + x_m}, \quad \Delta_{mv}^M = \frac{\epsilon_m x_v - \epsilon_v x_m}{\epsilon_m x_v + \epsilon_v x_m} \quad (4)$$

With $x_i^2 = x^2 + (\epsilon_i - \epsilon_v)(2h\omega_n/c)^2$, being c the speed of light. The subscripts m and v denote metal and vacuum, respectively. In these equations, the magnetic susceptibilities of the media have been assumed to be equal to unity. The ϵ_i is the dielectric response of each medium i , which reflects the tendency of that substance to polarize reacting to an electromagnetic wave. It is thus a function of the frequency of the incoming wave, which is also the frequency at which the particles of that material will oscillate in response³. Here the $\epsilon_i(\omega_n)$ are evaluated at the discrete set of Matsubara frequencies $\omega_n = 2\pi n k_B T/\hbar$, being \hbar the Planck's constant in units of angular frequency.

Notice that the result of 3 greatly generalizes the well known result of Casimir, and allows for a panoply of interaction, including non-monotonous dependence of $A_{ham}(h)$, as well as monotonic repulsive interactions. For instance, retardation-driven repulsion has been found for the force between gold and silica surfaces immersed in bromobenzene^{27,46}. This repulsive interaction in the Casimir regime has been found to allow supersliding between two surfaces, arising from an extremely low friction coefficient⁴⁷.

The prime in Eq. 3 means that the first term of the summation in n has half weight. This term corresponds to the contribution of the zero frequency, the only one that remains as $h \rightarrow \infty$, and it thus provides the interaction coefficient for very large distances. Singling out this term, the zero frequency contribution is given as⁴⁵:

$$A_{ham}^{\omega_n=0} = \frac{3k_B T}{4} \sum_{k=1}^{\infty} \left(\frac{\epsilon_m(0) - \epsilon_v(0)}{\epsilon_m(0) + \epsilon_v(0)} \right)^{2k} \frac{1}{k^3} \quad (5)$$

Where $\epsilon_i(0)$ is the static dielectric response, which for metals goes to infinity. Consequently, Eq. 5 reveals that the interaction of two plates of metal across vacuum has $A_{ham}^{\omega_n=0} = A_{ham}(h \rightarrow \infty) = \frac{3k_B T}{4} \zeta(3)$, which, at $T = 300$ K amounts to 3.73×10^{-21} J.

After these considerations, we can focus on the remaining contributions of Eq. 3, namely $A_{ham}^{\omega_n > 0}(h)$. A usual treatment of the Hamaker function is to consider only the first term of the summation in k^{48-51} . This is called the linear or dipole approximation, and works well in those cases where the $(\Delta_{mv}^E)^{2k} + (\Delta_{mv}^M)^{2k}$ function vanishes rapidly. In the situation that we handle, the large values of $\epsilon_m(\omega_n)$, specially for low frequencies due to the plasma resonance, make the use of the linear approximation unreliable.

Additionally, the complex interplay between London and Casimir regime that we have described is encapsulated inside the Eq. 3 in a non trivial way. In previous works^{41,42} we have taken advantage of several mathematical tools to provide insightful expressions within the linear approximation attempting to clarify the physical interpretation of the Lifshitz formula.

III. WQA BEYOND THE DIPOLE APPROXIMATION

The Weighted Quadrature Approximation (WQA) introduced recently within the linear dipole approximation⁴¹, employs the Gaussian Quadrature as an analytical tool to simplify the Lifshitz formula. Here we use the same idea to generalize the WQA to the infinite order sum of Eq. 3. After a first Gaussian Quadrature, using xe^{-kx} as the weight function, and the approximation of the summation in n to an integral via the Euler-MacLaurin formula, we reach⁴⁵

$$A_{ham}^{\omega_n > 0}(h) = \frac{3c\hbar}{8\pi} \int_{\nu_T}^{\infty} d\nu \sum_{k=1}^{\infty} \tilde{R}_k(\nu, x_{1,k}, h) [k\nu h + 1] e^{-k\nu h} \quad (6)$$

Where $\nu_T = 2\epsilon_v^{1/2}\omega_T/c$, $\omega_T = 2\pi k_B T/\hbar$ and $\tilde{R}_k(\nu, x_{1,k}, h) = \epsilon_v^{-1/2} j_v^{-1} R_k(\nu, x_{1,k}, h)$, being $j_v = \left(1 + \frac{1}{2} \frac{d \ln \epsilon_v}{d \ln \omega_n}\right)$, $x_{1,k} = (kr_n^2 + 2r_n + 2/k)/(kr_n + 1)$, and

$$R_k(\nu, x, h) = \frac{(\Delta_{mv}^E)^{2k} + (\Delta_{mv}^M)^{2k}}{k^3} \quad (7)$$

In practice, for metallic plates interacting across vacuum, $\epsilon_v(\omega) = 1$, so that $j_v = 1$, and $\tilde{R}_k(\nu, x, h) = R_k(\nu, x, h)$.

Recall that the dependence on $\nu = \nu_T n$, x , and h enters by the hand of $\Delta_{mv}^{E,M}$, as dictated by Eq. 4. The function $R_k(\nu, x, h)$ exhibits a very complicated dependence on the distance of separation, arising from the fact that the frequencies captured by the integral in Eq. 6 are being reduced as the distance increases. At this stage, this result is still too arid to infer intuitively the expected functional behavior.

We proceed by introducing ν_∞ , an effective parameter specific of each system meant to describe the decay length of $R_k(\nu, x, h)$ as $\nu \rightarrow \infty$. Then a second Gaussian

Quadrature is performed⁴⁵, and we achieve the WQA extended to include the complete summation over k

$$A_{ham}^{\omega_n > 0}(h) = \frac{3c\hbar\nu_\infty}{8\pi} \sum_{k=1}^{\infty} \tilde{R}_k(\nu_k^*, x_{1,k}, h) e^{\xi_k} e^{-\nu_T kh} \tilde{F}_k \quad (8)$$

$$\tilde{F}_k = \frac{(\nu_T kh + 1)(\nu_\infty kh + 1) + \nu_\infty kh}{(\nu_\infty kh + 1)^2}$$

$$\xi_k = \frac{(\nu_T kh + 1)(\nu_\infty kh + 1) + 2\nu_\infty kh}{(\nu_\infty kh + 1)^2(\nu_T kh + 1) + (\nu_\infty kh + 1)\nu_\infty kh}$$

With $\xi_k = (\nu_k^* - \nu_T)/\nu_\infty$.

Truncating the sum in Eq.8 beyond $k = 1$, this result becomes the original WQA proposed recently⁴¹. To this order of approximation, WQA is very accurate for dielectric materials with low dielectric response^{41,42}. However, the extension provided here is required to describe interactions for materials with large dielectric response, because the terms $\Delta_{mv}^{M/E}$ are close to unity and the convergence of the series is not fast enough to warrant truncation at first order.

Equation 8 has not only the advantage of being entirely analytic, but also allows straightforward interpretation of the transition from London to Casimir regime of $A_{ham}(h)$ through the comparison of the magnitudes of h , ν_∞ and ν_T .

For short distances, $h \ll \nu_\infty^{-1}$, we find the auxiliary functions $\tilde{F}_k = 1$ and $\xi_k = 1$, so that

$$A_{ham}^{\omega_n > 0}(h \rightarrow 0) = \frac{3c\hbar\nu_\infty}{8\pi} \sum_{k=1}^{\infty} \left(\frac{\epsilon_m - 1}{\epsilon_m + 1}\right)^{2k} \frac{e}{k^3} \quad (9)$$

with the dielectric function evaluated at a constant wave number $\nu^* = \nu_T + \nu_\infty$. Accordingly, the value of $A_{ham}(h \rightarrow 0)$ in Eq. 8 becomes independent of h , and the usual Hamaker constant is recovered. At large values of the distance of separation $h \gg \nu_T^{-1}$, we find $\xi_k \rightarrow 0$, while $\tilde{F}_k = \nu_T/\nu_\infty$. This yields:

$$A_{ham}^{\omega_n > 0}(h \rightarrow \infty) = \frac{3c\hbar\nu_T}{4\pi} \sum_{k=1}^{\infty} \left(\frac{\epsilon_m^{1/2} - 1}{\epsilon_m^{1/2} + 1}\right)^{2k} \frac{e^{-\nu_T kh}}{k^3} \quad (10)$$

where the dielectric functions are now evaluated at the thermal wave-number ν_T . In this limit, the retarded interactions are suppressed exponentially. Accordingly, only the static term in the Hamaker constant survives. This leads to the other asymptotic behavior $A_{ham}(h \rightarrow \infty)$, also independent of h . In between these two limits, $\nu_\infty^{-1} \ll h \ll \nu_T^{-1}$, the h dependence of $A_{ham}(h)$ is governed by the factor $\tilde{F}_k(h)$, which in this range effectively decays as $2/(\nu_\infty kh)$. This leads to:

$$A_{ham}^{\omega_n > 0}(h) = \frac{3c\hbar}{4\pi h} \sum_{k=1}^{\infty} \frac{(\Delta_m^E)^{2k} + (\Delta_m^M)^{2k}}{k^4} \quad (11)$$

where the dielectric functions are now to be evaluated at frequencies lying between ν_T and ν_∞ . For a perfect metal, implying $\Delta_{mv}^{E/M} = 1$, Eq.8 readily yields $A_{ham}^{\omega_n > 0}(h) = \frac{3c\hbar}{2\pi h} \zeta(4)$, which corresponds to the exact result of Casimir for two interacting metals at zero temperature.

This inspection highlights one major strength of the WQA: it provides a parametric clarification of the qualitative change of the distance dependence on the dispersion forces. The distance implied in ν_∞^{-1} signals the point at which the surface van der Waals free energy in Eq. 1 switches its dependence on the distance of separation from the $\sim 1/h^2$ proper of London regime, to the $1/h^3$ characteristic of Casimir interactions which is exact at zero temperature. At finite temperature, however, ν_T is finite, and the Casimir regime becomes fully suppressed for $h > \nu_T^{-1}$.

IV. A SIMPLE QUADRATURE METHOD FOR THE HAMAKER CONSTANT

For practical matters, use of Eq. 8 requires knowledge of the system's parameter ν_∞ , which must be chosen so as to obtain optimal agreement with the exact results. A look at the limiting regimes of $A_{ham}^{\omega_n > 0}(h)$ displayed in Eq.9-11 shows that the choice of ν_∞ is only significant in the limit of small h . Accordingly, we seek ν_∞ by matching the $h \rightarrow 0$ limit of Eq. 8 to the exact $A_{ham}^{\omega_n > 0}(0)$ from Eq. 3 (c.f. Ref.⁴²). Unfortunately, the numerical calculation of $A_{ham}^{\omega_n > 0}(0)$ also is a cumbersome task. Therefore, in this section we present a very accurate one-point quadrature for $A_{ham}(0)$ that adopts a particularly simple analytic form for two metallic plates obeying the Drude model.

Our starting point is Eq.6 in the limit of $h \rightarrow 0$:

$$A_{ham}^{\omega_n > 0}(h \rightarrow 0) = \frac{3c\hbar}{8\pi} \int_{\nu_T}^{\infty} d\nu Li_3(R_1) \quad (12)$$

where $Li_3(x) = \sum_{k=1}^{\infty} x^k/k^3$ is the polylogarithmic function, and $R_1(\nu) = R_1(\nu, x, h = 0)$ takes the particularly simple form:

$$R_1(\nu) = \left(\frac{\epsilon_m(i\nu) - \epsilon_v(i\nu)}{\epsilon_m(i\nu) + \epsilon_v(i\nu)} \right)^2 \quad (13)$$

Analytical approximations for the Hamaker constant are usually obtained by replacing $Li_3(R_1)$ by its zeroth order approximation $Li_3(R_1) \approx R_1$ and truncating beyond first order. Here, we notice that $R_1(\nu)$ has the properties of a well behaved distribution, so that applying the first mean value theorem, Eq.12 may be expressed exactly as:

$$A_{ham}^{\omega_n > 0}(h \rightarrow 0) = \frac{3c\hbar}{8\pi} \frac{Li_3(R_1^*)}{R_1^*} \int_{\nu_T}^{\infty} d\nu R_1(\nu) \quad (14)$$

where $R_1^* = R_1(\nu^*)$, is evaluated at a mean value frequency, ν^* , in the interval between ν_T and ∞ . An accurate estimate of R_1^* , without needing an explicit evaluation of ν^* may be obtained right away by requiring the

second order expansion of the quadrature rule Eq.14 to match exactly that of Eq.12. This then leads to the simplified prescription (see supplementary material, Ref.⁴⁵):

$$A_{ham}^{\omega_n > 0}(h \rightarrow 0) = \frac{Li_3(R_1^*)}{R_1^*} A_{ham,0}^{\omega_n > 0} \quad (15)$$

where

$$R_1^* = \frac{I_2}{I_1}, \quad I_m = \int_{\nu_T}^{\infty} [R_1(\nu)]^m d\nu$$

while $A_{ham,0}^{\omega_n > 0} = \frac{3c\hbar}{8\pi} I_1$ is just the usual zeroth order approximation of the Hamaker constant.

In practice, $R_1(\nu) < 1$ at all frequencies, so that R_1^* is small always and $Li_3(R_1^*)/R_1^* = 1 + R_1^*/8 + (R_1^*)^2/27 \dots$ is a correction factor of order unity. In fact, by construction, Eq.15 is exact up to second order in R_1^* , and provides very accurate results when compared with the numerical solution of Eq. 3. Henceforth, we will refer to the prescription of Eq.15 as the Q rule. Its performance will be tested later for the interaction between two plates of Al, Be, Cr, W and Au using recently published data as a benchmark.^{43,44}

V. ANALYTIC SOLUTION FOR THE DRUDE MODEL

In the following, we will gauge Eq.8 at $h = 0$ with Eq.15 in order to estimate the system parameter ν_∞ . Once this is known, we can then use Eq.8 to estimate the Hamaker function for arbitrary values of the plate separation.

We begin the exploitation of the previous formulae by assuming the single - Drude model - oscillator as a sufficient description of the dielectric response of the metal. This model assumes free moving electrons⁵², i.e. electrons displacing with no restoring force³, oscillating at the plasma frequency, ω_P . These electrons can experience collisions with defects, lattice vibrations or with other electrons⁵³, resulting in a damping coefficient, γ . All together, the Drude model reads

$$\epsilon_m(i\omega) = 1 + \frac{\omega_P^2}{\gamma\omega + \omega^2} \quad (16)$$

This representation has a fundamental limitation. It is not clear that the employment of the Drude model for real metals is physically justified, since most of them are expected to exhibit interband transitions⁵⁴. This might be surpassed simply by considering that the Drude model is merely a phenomenological description of $\epsilon_m(i\omega)$, which is always a smooth function irrespective of the complex optical response of the metal.

It is with such spirit that Ordal *et al.* published⁵⁴ a set of Drude model parameters for various metals obtained from a fit of data in the near and far IR regime. These parameters are tabulated in Table I for Al, W, Ag and Pb,

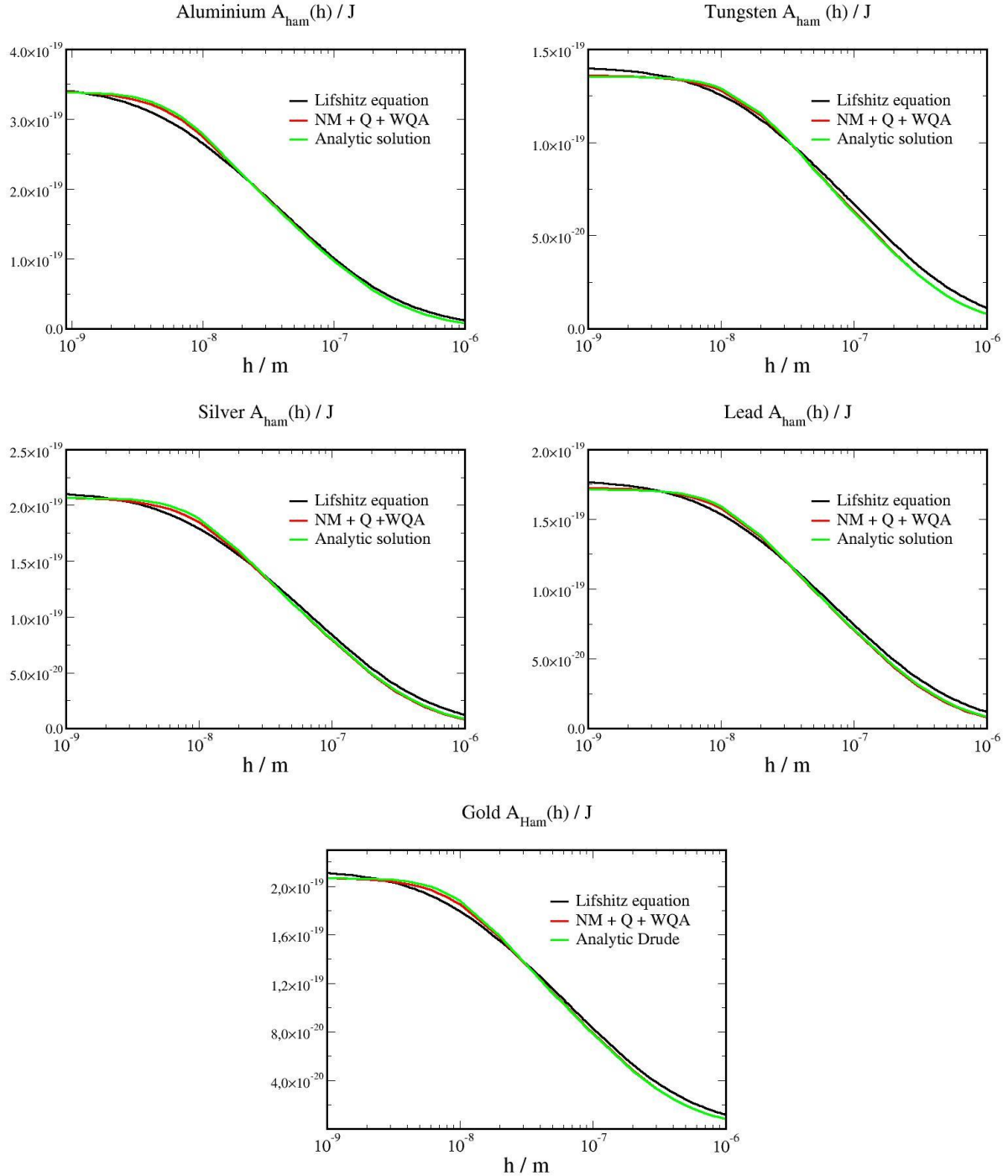


FIG. 1: Retarded interaction coefficients computed with the Drude model at 300 K. Hamaker coefficients for the interaction of two plates of Al (top left), W (top right), Ag (bottom left) and Pb (bottom right), across vacuum. The $A_{ham}(h)$ are displayed in Joules. In each case, it is shown a comparison of the $A_{ham}(h)$ resulting from the Lifshitz equation (Eq. 3) in black, the WQA with ν_∞ obtained via the Numerical Method to match the Quadrature $A_{ham,Q}(0)$ (NM + Q + WQA) in red, and the WQA supported by the analytic solution for ν_∞ in green.

which also includes results from Gudarzi and Aboutalebi for Au⁴⁴.

However, it is clear that the Drude model does not properly account for the possible contributions of the high

frequencies. This potentially has a great impact on the calculations surrounding the Lifshitz theory, because most of the Matsubara frequencies fall on a high energy regime. Even if the fact that metals are good conductors

entails that the IR frequencies will strongly contribute to $A_{ham}(h)$, neglecting the remaining frequencies might provide a poor estimation. Hence the consequences of performing such approximation will be discussed later.

Nevertheless, the use of the Drude model presents a very important advantage: it allows us to get an explicit expression of ν_∞ for the interaction between two plates of a certain metal across vacuum, depending fundamentally on the plasma frequency of that metal⁴⁵. Indeed, assuming $\omega_P \gg \gamma, \omega_T$, which is usually the case, Eq.15 provides the following simple result for the Hamaker constant between two metallic plates:

$$A_{ham}^{\omega_n > 0}(h \rightarrow 0) = \frac{3 Li_3(5/8)}{5\sqrt{8}} \hbar \omega_P \quad (17)$$

Matching this result to the $h \rightarrow 0$ limit of Eq.8 provides a transcendental equation for ν_∞ which can be solved exactly to yield:

$$\nu_\infty = f\nu_P - \nu_T \quad (18)$$

Where $\nu_P = \frac{2}{c}\omega_P$ and $f = 0.553656$. Using Eq.18 together with Eq.8 provides a fully analytical description of the Hamaker function in all ranges of plate separation. We test this result for a number of metals. The analytical solution is compared with two numerical estimates of different level or refinement. Firstly, results are compared with the exact Hamaker function of Eq.3. Secondly, results are given for the WQA, Eq.8, with the parameter ν_∞ obtained by forcing $A_{ham}^{\omega_n > 0}(h \rightarrow 0)$ of the WQA (Eq.8) to match $A_{ham,Q}^{\omega_n > 0}(h \rightarrow 0)$ of the Quadrature in Eq. 15. We call the latter prescription the NM + Q + WQA method. Table I displays values of ν_∞ that result from this prescription for a number of metals.

Fig. 1 illustrates the results of this comparison. The analytic solution shows excellent agreement with the two numerical methods for all tested metals, which highlights the accuracy of our closed form results Eq.8 and Eq.17-Eq.18.

	<i>Al</i>	<i>W</i>	<i>Ag</i>	<i>Pb</i>	<i>Au</i>
ω_P/eV	14.78	6.01	9.01	7.70	9.1
$\gamma \cdot 10^2/eV$	8.04	5.38	1.80	18	6.0
$\nu_\infty \cdot 10^{-7}/m^{-1}$	3.80	1.56	2.32	2.00	9.27

TABLE I: Plasma frequency, ω_P , and damping coefficient, γ used in this work. Results for Al, W, Ag and Pb from Ref.⁵⁴. Results for Au from Ref.⁴⁴. The last line shows the ν_∞ parameter obtained with the Numerical Method, employed to get the red lines in Fig. 1.

To check whether the Drude model is adequate enough to account for a complete description of $\epsilon_m(\omega)$, we take advantage of improved dielectric parametrizations reported recently, which account for interband transitions

in the ultraviolet frequencies and beyond.^{43,44} We use this data to compute the retarded Hamaker coefficients with the Lifshitz equation, and compare it with the output of the analytic solution for a single Drude oscillator.

Fig.2 displays $A_{ham}(h)$ of Al and W emerging from Eq. 3 with the parameterization of P. Tolias⁴³, compared to the output of the analytic expression with the Drude model using the parameters published by Ordal *et al*⁵⁴. In the case of Al, the Drude model seems to provide a good characterization of $\epsilon_m(\omega)$, resulting in a very similar $A_{ham}(h)$ function for all separation distances.

On the contrary, for W, the high frequencies contributions to $A_{ham}(h)$ that are missed by the single Drude fit lead to a very low estimate of the Hamaker constant as obtained from the analytic solution. As the retardation effect sets in, these large frequencies are cut off, and the remaining ones are properly given by the Drude model, so that the very large distances regime is well described with the single oscillator model of Ordal *et al*. This highlights that the analytic solution will provide a poor approximation whenever the metal presents significant high frequency contributions to its dielectric response, revealing an insufficiency of the Drude model to account for those frequencies.

This observation is relevant for the experimental measurement of the Casimir regime of van der Waals forces.²⁴⁻²⁹ Particularly, high precision experiments aimed at testing the low temperature limit, Eq.2 often rely on the asymptotic expansion of Eq.3 based on a single Drude oscillator. It is therefore very important to assess to what extent can one neglect contributions of interband transitions of small wave-length. We check this for the particularly significant case of gold, which is most often the choice for high precision measurements of the Casimir force.²⁴⁻²⁹ Fig.3 displays the exact Lifshitz result for gold, with dielectric properties as obtained in Ref.⁴⁴ The black line is the result obtained with the complete dielectric response, while the blue line provides the Hamaker function when only the conducting electrons are considered. At short distances, we see that more than half of the Hamaker constant results from contributions due to core electrons, as expected. Starting at about 100 nm, however, the contribution of core electrons has vanished almost completely. Whence, for gold it appears that asymptotic expansions based on simple Drude or plasma models should be reliable in the micrometer range. Care must be taken when asymptotic expansions are used below the hundredth of nanometer range, however.

VI. COMPARISON WITH NUMERICAL SOLUTIONS

So far we have tested the Quadrature proposed in Eq. 15 for metals described by the Drude model, where the integrals implied by I_m are analytically solvable⁴⁵.

As demonstrated in the preceding section, despite of

its potential strength, the use of the analytic solution of the Drude model is quite circumstantial, depending on whether the high energy regime is negligible or not.

Now we show that the single-point quadrature of Eq.15 alone is able to provide a simple method to get the Hamaker constant, $A_{ham}(0)$, upon numerical integration, even for those cases where $\epsilon_m(\omega)$ exhibits a complex high-frequency behavior. We use once again the fits for the dielectric response of metals published by Tolia and Gardarzi and Aboutalebi to get the I_1 and I_2 appearing in Eq. 15 through numerical integration with the composite trapezoidal rule.^{43,44}

	<i>Al</i>	<i>W</i>	<i>Be</i>	<i>Cr</i>	<i>Au</i>
$A_{ham,Q}(0)/(10^{-19} J)$	3.44	4.74	3.39	3.61	4.40
$A_{ham}(0)/(10^{-19} J)$	3.53	4.85	3.47	3.69	4.49
r. e. %	2.55	2.27	2.30	2.17	2.00

TABLE II: Hamaker constants for several metals as obtained from detailed optical properties of Ref.^{43,44}. The first line displays the Quadrature values computed with numerical integration, where

$A_{ham,Q}(0) = A_{ham,Q}^{\omega_n > 0}(0) + A_{ham,Q}^{\omega_n = 0}$. The second line shows exact results from Lifshitz theory. Results for Al, W, Be, Cr from Ref.⁴³. Results for Au calculated in this work using a dielectric functions as provided in Ref.⁴⁴.

The last line contains the relative error made by the Quadrature method.

Fig.4 represents the Hamaker function of Al, comparing the result of the exact Lifshitz equation with the NM+Q+WQA prescription (Eq.8 and Eq.15). We plot in dashed purple lines the solution of Eq. 8 including an increasing number of terms in the summation over k to check the convergence of the series. The second term provides already acceptable accuracy with respect to the complete summation, and almost complete convergence is achieved with the third term. This examination supports the use of a Quadrature exact up to second order, that was the assumption under which Eq. 15 was derived. In fact, the difference between the second order ($k = 2$) and third order results ($k = 3$) is smaller than the uncertainty that results from the parameterization of the dielectric response in most systems⁵⁵.

When numerically solving the equality between $A_{ham,Q}^{\omega_n > 0}(h \rightarrow 0)$ of the Quadrature and $A_{ham}^{\omega_n > 0}(h \rightarrow 0)$ of the WQA for tungsten, it was found that there is no ν_∞ parameter that provides exactly that match. In this case, the validity of the Q+WQA method can be compromised. In practice, we find that taking the parameter that gives the larger possible $A_{ham}^{\omega_n > 0}(h \rightarrow 0)$ already results in a very good approximation for both the value of the Hamaker constant and the habit of the Hamaker function in the Casimir regime. Indeed, the Fig. 4 shows that the WQA reproduces closely the functional behavior of the Hamaker function of the Lifshitz theory. We found that this problem does

become quite significant for the relevant case of gold. Here, we did not find a choice of ν_∞ that could match the Hamaker constant, and the optimal value provides a Hamaker function that underestimates $A_{ham}(h \rightarrow 0)$ by 15%, as shown in Fig.3.

Despite this deficiency in predicting the full Hamaker function for some metals, the proposed method for the calculation of Hamaker constants does remarkably well for all metals studied. Table II displays the comparison between Hamaker constants of Al, W, Be, Cr and Au, and those obtained via Eq. 15. The Quadrature provides good agreement with the result of the Lifshitz equation without retardation, and its performance never exceeds a 3% of relative error. This suggests the use of this novel Quadrature as a straightforwardly solvable alternative to the more intricate Lifshitz formula. The use of this formula is expected to be particularly helpful for estimating Hamaker constants between materials across a dielectric medium, where the first order approximation or Tabor-Winterton approximation often fails⁵¹.

VII. CONCLUSIONS

Understanding the dispersive interactions between two surfaces is a crucial feature in the study of adhesion and friction phenomena^{2,3,27}. At zero temperature, the van der Waals free energy exhibits a crossover from the non-retarded (London) behavior at short distances to the retarded (Casimir) behavior at long distances of separation²⁰. At finite temperature, however, the Casimir regime of retarded interactions is suppressed at sufficiently large distances. This complex crossover behavior is non-trivially embodied in the Lifshitz equation for retarded interactions. The influence of the retardation effect switches the distance dependence of the interaction energy from the $\sim 1/h^2$ typical of London dispersion interaction, to the $\sim 1/h^3$ associated to the Casimir regime³ and back to $\sim 1/h^2$ at finite temperature and inverse distances smaller than a thermal wave-number ν_T .

In this paper, we have worked out an analytical approximation for the Hamaker function which illustrates the crossover behavior between these three different regimes and remains accurate at all ranges of separation. In this study, we also present an accurate Quadrature method to compute the Hamaker constant corresponding to the limit of small plate separation. Our quadrature rule consistently reproduces the values of $A_{ham}(0)$ provided by previous studies⁴³, with less than 3% error. We have illustrated our results with the special case of two metallic plates in vacuum, but the method can be applied just as well for any two materials interacting across a dielectric medium.

Finally, we made use of the Quadrature method to infer a fully analytical equation for the computation of the retarded interaction coefficients between two metal plates

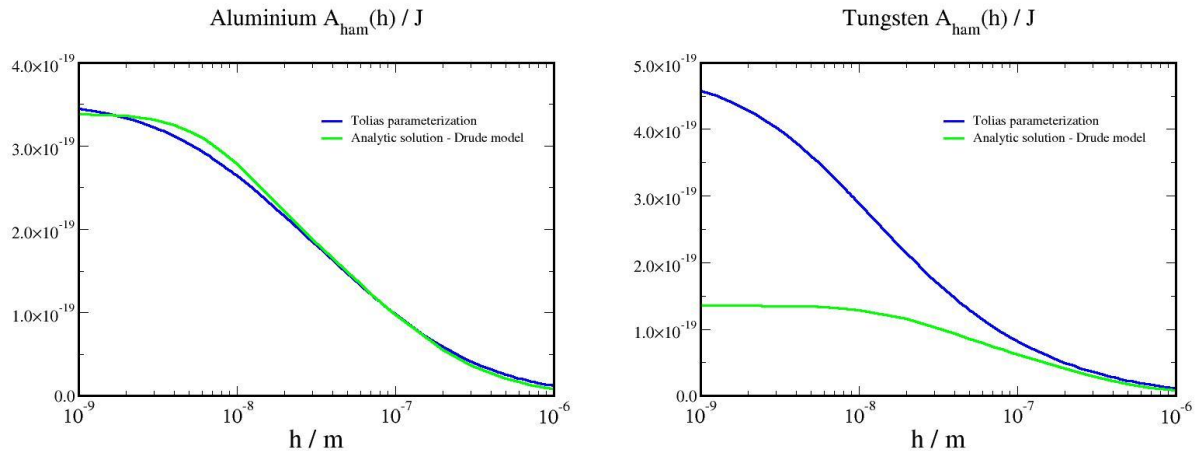


FIG. 2: Retarded interaction coefficients of several metals at 300 K. The blue lines represent the Hamaker coefficients for the interaction of Al (left), and W (right), using the Lifshitz equation and detailed dielectric data from Ref.⁴³. The analytic solution within the Drude model is also displayed in green for comparison. The Hamaker coefficients are provided in Joule.

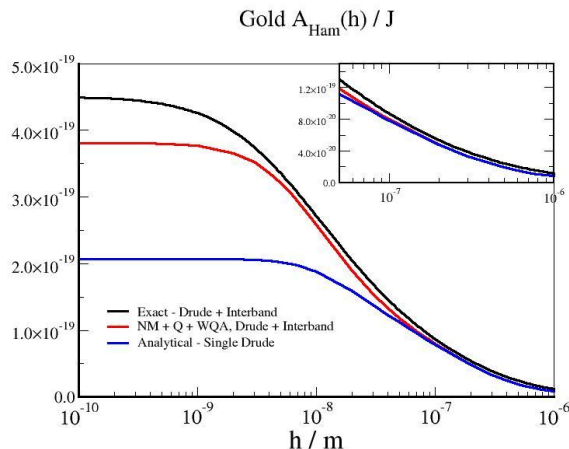


FIG. 3: $A_{ham}(h)$ for the interaction of gold plates across air. The black line is obtained using Lifshitz theory, with full dielectric properties as reported in Ref⁴⁴ (Drude oscillator + core electrons). The blue line are results obtained using only the Drude oscillator for conduction electrons. The red line is predictions from NM + Q + WQA for the full dielectric response.

with dielectric response as given by a single Drude oscillator. However, we highlight that the use of this formula is limited to those metals with little response at large frequencies.

We believe that this work provides a comprehensive picture of the behavior of the retarded interactions between metallic plates. Methodologically, we hope that the quadrature rules employed here are susceptible of quantitative exploitation in a broad range of studies where dispersion interactions play an important role.

ACKNOWLEDGMENTS

We acknowledge funding from the Spanish Agencia Estatal de Investigación under grant FIS2017-89361-C3-2-

P.

AUTHORS CONTRIBUTIONS

JLM and LGM discussed and formulated theory. JLM performed calculations and drafted manuscript. LGM designed research and revised manuscript.

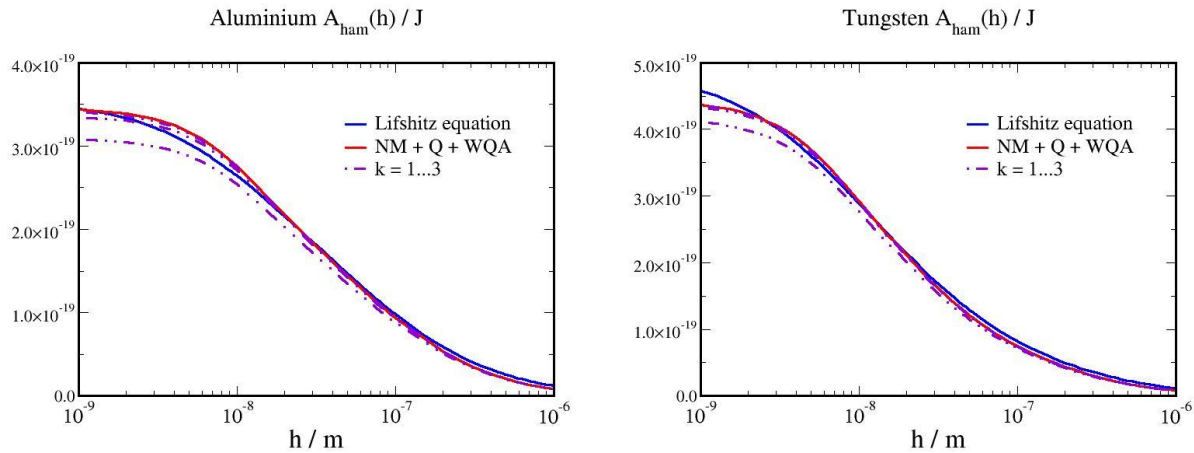


FIG. 4: $A_{ham}(h)$ of Aluminium (left) and Tungsten (right) resulting from the Lifshitz formula (blue line) and the WQA (red line), with detailed optical properties as described in Ref.⁴³. The ν_∞ parameter of the WQA has been obtained via Numerical Method to match the Quadrature, and the dashed violet lines represent the WQA solution with one, two, and three terms of the summation in k . Hamaker functions are provided in Joule.

- * juan.luengo@uam.es
† lgmac@quim.ucm.es
- ¹ B. Derjaguin, *Langmuir* **3**, 601 (1987).
 - ² J. N. Israelachvili, *Intermolecular and Surfaces Forces*, 2nd ed. (Academic Press, London, 1991).
 - ³ V. A. Parsegian, *Van der Waals Forces* (Cambridge University Press, Cambridge, 2005) pp. 1–311.
 - ⁴ B. W. Ninham and P. L. Nostro, *Molecular Forces and Self Assembly: In Colloids, Nanoscience and Biology* (Cambridge University Press, Cambridge, 2010).
 - ⁵ J. Fiedler, M. Boström, C. Persson, I. Brevik, R. Corkery, S. Y. Buhmann, and D. F. Parsons, *J. Phys. Chem. B* **124**, 3103 (2020), pMID: 32208624, <https://doi.org/10.1021/acs.jpcc.0c00410>.
 - ⁶ V. Estes, S. Carretero-Palacios, L. G. MacDowell, J. Fiedler, D. F. Parsons, F. Spallek, H. Míguez, C. Persson, S. Y. Buhmann, I. Brevik, and M. Boström, *Phys. Chem. Chem. Phys.* **22**, 11362 (2020).
 - ⁷ V. Parsegian and B. Ninham, *Nature* **224**, 1197 (1969).
 - ⁸ K. Autumn, Y. A. Liang, S. T. Hsieh, W. Zesch, W. P. Chan, T. W. Kenny, R. Fearing, and R. J. Full, *Nature* **405**, 681 (2000).
 - ⁹ H. Hamaker, *Physica* **4**, 1058 (1937).
 - ¹⁰ S. Dietrich, in *Phase Transitions and Critical Phenomena*, Vol. 12, edited by C. Domb and J. L. Lebowitz (Academic, New York, 1988) pp. 1–89.
 - ¹¹ M. Schick, in *Liquids at Interfaces*, Les Houches Lecture Notes (Elsevier, Amsterdam, 1990) pp. 1–89.
 - ¹² I. E. Dzyaloshinskii, E. M. Lifshitz, and L. P. Pitaevskii, *Soviet Physics Uspekhi* **4**, 153.175 (1961).
 - ¹³ E. M. Lifshitz, *Soviet Phys.* **2**, 73 (1956).
 - ¹⁴ H. B. Casimir, in *Proc. Kon. Ned. Akad. Wet.*, Vol. 51 (1948) p. 793.
 - ¹⁵ J. N. Israelachvili and D. Tabor, *Proceedings of the Royal Society of London A: Mathematical, Physical and Engineering Sciences* **331**, 19 (1972), see white76,chan77, <http://rspa.royalsocietypublishing.org/content/331/1584/19.full.pdf>.
 - ¹⁶ E. S. Sabisky and C. H. Anderson, *Phys. Rev. A* **7**, 790 (1973).
 - ¹⁷ L. R. White, J. N. Israelachvili, and B. W. Ninham, *J. Chem. Soc., Faraday Trans. 1* **72**, 2526 (1976).
 - ¹⁸ D. Chan and P. Richmond, *Proc. R. Soc. Lond. A* **353**, 163 (1977), <http://rspa.royalsocietypublishing.org/content/353/1673/163.full.pdf>.
 - ¹⁹ J. Gregory, *J. Colloid. Interface Sci.* **83**, 138 (1981).
 - ²⁰ G. Palasantzas, P. Van Zwol, and J. T. M. De Hosson, *Applied Physics Letters* **93**, 121912 (2008).
 - ²¹ P. J. van Zwol and G. Palasantzas, *Phys. Rev. A* **81**, 062502 (2010).
 - ²² K. Milton, in *The Casimir Effect 50 Years Later*, edited by M. Bordag (World Scientific, Singapore, 1998) pp. 507–542.
 - ²³ S. K. Lamoreaux, *Phys. Today* **60**, 40 (2007).
 - ²⁴ S. K. Lamoreaux, *Phys. Rev. Lett.* **78**, 5 (1997).
 - ²⁵ U. Mohideen and A. Roy, *Phys. Rev. Lett.* **81**, 4549 (1998).
 - ²⁶ G. Bressi, G. Carugno, R. Onofrio, and G. Ruoso, *Phys. Rev. Lett.* **88**, 041804 (2002).
 - ²⁷ J. N. Munday, F. Capasso, and V. A. Parsegian, *Nature* **457**, 170 (2009).
 - ²⁸ S. de Man, K. Heeck, R. J. Wijngaarden, and D. Iannuzzi, *Phys. Rev. Lett.* **103**, 040402 (2009).
 - ²⁹ J. L. Garrett, D. A. T. Somers, and J. N. Munday, *Phys. Rev. Lett.* **120**, 040401 (2018).
 - ³⁰ J. M. Obrecht, R. J. Wild, M. Antezza, L. P. Pitaevskii, S. Stringari, and E. A. Cornell, *Phys. Rev. Lett.* **98**, 063201 (2007).
 - ³¹ L. Fisher and B. Ninham, arXiv: Quantum Physics (2020).
 - ³² B. W. Ninham and V. A. Parsegian, *Biophys. J.* **10**, 646 (1970).
 - ³³ V. A. Parsegian and B. W. Ninham, *Biophys. J.* **10**, 664 (1970).

- ³⁴ J. Schwinger, L. L. DeRaad, and K. A. Milton, *Ann. Phys.* **115**, 1 (1978).
- ³⁵ B. W. Ninham and J. Daicic, *Phys. Rev. A* **57**, 1870 (1998).
- ³⁶ M. Boström and B. E. Sernelius, *Phys. Rev. Lett.* **84**, 4757 (2000).
- ³⁷ A. Lambrecht and S. Reynaud, *Euro. Phys. J. D* **8**, 309 (2000).
- ³⁸ V. B. Bezerra, G. L. Klimchitskaya, V. M. Mostepanenko, and C. Romero, *Phys. Rev. A* **69**, 022119 (2004).
- ³⁹ B. Geyer, G. L. Klimchitskaya, and V. M. Mostepanenko, *Phys. Rev. B* **72**, 085009 (2005).
- ⁴⁰ B. W. Ninham, M. Bostrom, C. Persson, I. Brevik, S. Y. Buhmann, and B. E. Sernelius, *Euro. Phys. J. D* **68** (2014).
- ⁴¹ L. G. MacDowell, *J. Chem. Phys.* **150**, 081101 (2019).
- ⁴² J. Luengo-Márquez and L. G. MacDowell, *Journal of Colloid and Interface Science* **590**, 527 (2021).
- ⁴³ P. Tolias, *Fusion Engineering and Design* **133**, 110 (2018).
- ⁴⁴ M. M. Gudarzi and S. H. Aboutalebi, *Sci. Adv.* **7**, eabg2272 (2021), <https://www.science.org/doi/pdf/10.1126/sciadv.abg2272>.
- ⁴⁵ J. Luengo-Márquez and L. G. MacDowell, “Supplementary material,” (2021), retarded interactions between two metal plates.
- ⁴⁶ M. Boström, B. E. Sernelius, I. Brevik, and B. W. Ninham, *Phys. Rev. A* **85**, 010701 (2012).
- ⁴⁷ A. A. Feiler, L. Bergström, and M. W. Rutland, *Langmuir* **24**, 2274 (2008).
- ⁴⁸ D. Tabor and R. H. S. Winterton, *Proc. R. Soc. Lond. A* **312**, 435 (1969), <http://rspa.royalsocietypublishing.org/content/312/1511/435.full.pdf>.
- ⁴⁹ D. B. Hough and L. R. White, *Adv. Colloid Interface Sci.* **14**, 3 (1980).
- ⁵⁰ D. C. Prieve and W. B. Russel, *J. Colloid. Interface Sci.* **125**, 1 (1988).
- ⁵¹ L. Bergström, *Adv. Colloid Interface Sci.* **70**, 125 (1997).
- ⁵² S. Youn, T. Rho, B. Min, and K. S. Kim, *physica status solidi (b)* **244**, 1354 (2007).
- ⁵³ D. B. Tanner, *Optical Effects in Solids* (University of Florida, 2013).
- ⁵⁴ M. A. Ordal, L. Long, R. Bell, S. Bell, R. Bell, R. Alexander, and C. Ward, *Applied optics* **22**, 1099 (1983).
- ⁵⁵ F. A. Burger, R. W. Corkery, S. Y. Buhmann, and J. Fiedler, *The Journal of Physical Chemistry C* **124**, 24179 (2020), <https://doi.org/10.1021/acs.jpcc.0c06748>.

Supporting Information for
Analytical theory for the crossover from retarded to non-retarded interactions
between two metal plates

by

Juan Luengo-Márquez¹ and Luis G. MacDowell²

¹Department of Theoretical Condensed Matter Physics and Instituto Nicolás Cabrera,
Universidad Autónoma de Madrid, 28049 Madrid (Spain)

²Departamento de Química Física, Facultad de Ciencias Químicas, Universidad Complutense, Madrid, 28040, Spain.

This document contains supporting information on the derivation of results from the main paper. To facilitate cross referencing, this materials is written as an appendix section. The equation numbering and bibliography follow the original paper, with equation labels and references not in this document referring to those of the original paper.

Appendix A: Lifshitz equation with retardation

The Hamaker function of the exact Lifshitz equation for the interaction between two plates "1" and "2" composed of two arbitrary substances, across a medium "med" reads

$$A_{ham}(h) = -6h^2 k_B T \sum_{n=0}^{\infty}{}' \int_0^{\infty} \rho \, d\rho \ln(D^E D^M) \quad (\text{A1})$$

$$D^{E,M} = 1 - \Delta_{1med}^{E,M} \Delta_{2med}^{E,M} e^{-2\rho_{med} h}$$

$$\Delta_{imed}^E = \frac{\rho_{med} - \rho_i}{\rho_{med} + \rho_i}, \quad \Delta_{imed}^M = \frac{\epsilon_i \rho_{med} - \epsilon_{med} \rho_i}{\epsilon_i \rho_{med} + \epsilon_{med} \rho_i}$$

$$\rho_{i,med}^2 = \rho^2 + \frac{\epsilon_{i,med} \omega_n^2}{c^2}, \quad \omega_n = \frac{2\pi k_B T}{\hbar} n$$

Being T the temperature in Kelvin, k_B the Boltzmann constant, c the speed of light, \hbar the Planck constant in units of angular frequency, and h the separation between the two plates, i. e. the thickness of the medium in between. Where the prime after the summation means that the $n = 0$ term has an additional factor of 1/2. The dielectric responses, $\epsilon_{i,med}$, are evaluated at the discrete Matsubara frequencies, ω_n . Finally, $D^{E,M}$ expresses a condition imposed by the geometry of the system that every electromagnetic wave crossing through it must fulfill. When equalized to zero, it is dubbed the dispersion relation of the system.

After splitting $\ln(D^E D^M) = \ln(D^E) + \ln(D^M)$ in Eq. A1 and performing a Taylor expansion on each logarithm, we readily get

$$A_{ham}(h) = 6h^2 k_B T \sum_{n=0}^{\infty}{}' \int_0^{\infty} \rho \, d\rho \sum_{k=1}^{\infty} \frac{(\Delta_{1med}^E \Delta_{2med}^E)^k + (\Delta_{1med}^M \Delta_{2med}^M)^k}{k} e^{-2k\rho_{med} h} \quad (\text{A2})$$

We proceed now by changing the variable of the integral twice, first through $\rho \rightarrow \rho_{med}$, and then through $2\rho_{med} h \rightarrow x$. This procedure yields

$$A_{ham}(h) = \frac{3k_B T}{2} \sum_{n=0}^{\infty}{}' \int_{r_n}^{\infty} \sum_{k=1}^{\infty} x \, dx \frac{(\Delta_{1med}^E \Delta_{2med}^E)^k + (\Delta_{1med}^M \Delta_{2med}^M)^k}{k} e^{-kx} \quad (\text{A3})$$

$$r_n = \frac{2h\epsilon_{med}^{1/2}\omega_n}{c}$$

$$\Delta_{imed}^E = \frac{x_{med} - x_i}{x_{med} + x_i}, \quad \Delta_{imed}^M = \frac{\epsilon_i x_{med} - \epsilon_{med} x_i}{\epsilon_i x_{med} + \epsilon_{med} x_i}$$

$$x_i^2 = x^2 + (\epsilon_i - \epsilon_{med}) \left(\frac{2h\omega_n}{c} \right)^2$$

Note that Eq. 3 and 4 of the main text are recovered after particularizing for the specific system under consideration with $\epsilon_{med} = \epsilon_v$, $x_{med} = x_v$, $\epsilon_1 = \epsilon_2 = \epsilon_m$, and $x_1 = x_2 = x_m$. All along this Supplementary Material we will address the general notation employed so far to extend certain results to differently labelled geometries, but the particularization is straightforwardly derived after substitution of the previous equalities.

The Eq. 5 of the main text is achieved by separating the $n = 0$ term of Eq. A3. Then $x_{i,med} = x$, so that all Δ_{imed}^E vanish, and the term with Δ_{imed}^M becomes constant in x . The resulting integral is easily solvable, and we reach

$$A_{ham}^{\omega_n=0} = \frac{3k_B T}{4} \sum_{k=1}^{\infty} \left(\frac{\epsilon_1(0) - \epsilon_{med}(0)}{\epsilon_1(0) + \epsilon_{med}(0)} \right)^k \left(\frac{\epsilon_2(0) - \epsilon_{med}(0)}{\epsilon_2(0) + \epsilon_{med}(0)} \right)^k \frac{1}{k^3} \quad (\text{A4})$$

Where only the static dielectric responses appear, i. e. the responses at zero frequency.

Appendix B: Weighted Quadrature Approximation

The WQA takes advantage of the one point Gaussian Quadrature used as an analytical tool to compute the integrals in Eq. A3. Generally, as a numerical tool, the N points Gaussian Quadrature is written as:

$$\int_a^b f(x)w(x)dx = \sum_{i=1}^N f(x_i)m_i \quad (\text{B1})$$

Where the smooth function $f(x)$ is evaluated at the nodes x_i , and $w(x)$ is the weight function of the quadrature. The set of nodes and weights x_i, m_i are chosen such that the integrals

$$I_j = \int_a^b x^j w(x) dx$$

are exact up to order $2N - 1$. Then the one point Gaussian Quadrature simply yields

$$\int_a^b f(x)w(x)dx = f(x_1)m_1 \quad (\text{B2})$$

$$I_0 = \int_a^b w(x)dx, \quad I_1 = \int_a^b xw(x)dx$$

$$m_1 = I_0, \quad x_1 = \frac{I_1}{I_0}$$

We take the $\omega_n > 0$ contributions to $A_{ham}(h)$ in Eq. A3, and then define $w(x) = xe^{-kx}$ as the weight function. Thus we have that

$$I_0 = \int_{r_n}^{\infty} xe^{-kx} dx = \frac{(kr_n + 1)}{k^2} e^{-kr_n} \quad (\text{B3})$$

$$I_1 = \int_{r_n}^{\infty} x^2 e^{-kx} dx = \frac{(k^2 r_n^2 + 2kr_n + 2)}{k^3} e^{-kr_n}$$

From which we get the corresponding m_1 and x_1 . The integral in x in Eq. A3 is computed through the quadrature, and after extracting the summation in k we reach

$$A_{ham}^{\omega_n > 0}(h) = \frac{3k_B T}{2} \sum_{k=1}^{\infty} \sum_{n=1}^{\infty} R_k(n, x_{1,k}, h) [kr_n + 1] e^{-kr_n} \quad (\text{B4})$$

$$R_k(n, x, h) = \frac{(\Delta_{1med}^E \Delta_{2med}^E)^k + (\Delta_{1med}^M \Delta_{2med}^M)^k}{k^3}$$

$$x_{1,k} = \frac{kr_n^2 + 2r_n + 2/k}{kr_n + 1}$$

Recall that $\Delta_{imed}^{E,M} = \Delta_{imed}^{E,M}(n, x)$. Next we aim to approximate the summation in n to an integral, for what we compute first the first-order correction of the Euler-MacLaurin formula

$$F = \sum_{n=a}^b f(n) = \int_a^b f(n)dn + \frac{1}{2}(f(a) + f(b)) + \sum_{k=1}^{\infty} \frac{B_{2k}}{2k!} (f^{(2k-1)}(b) - f^{(2k-1)}(a)) \quad (B5)$$

$$\Delta F_{1st-order} = \frac{1}{2}(f(a) + f(b)) + \frac{1}{12}(f'(b) - f'(a))$$

Where B_i are the Bernoulli coefficients and $f^{(2k-1)}(n)$ represents the $(2k-1)$ th derivative of $f(n)$. Note that the algebraic evolution of $R_k(n, x, h)$ in n can be taken as constant compared to the exponential decay of $(kr_n - 1)e^{-kr_n}$. Under this consideration, the computation of the first-order correction term of the Euler-MacLaurin formula for $f(n) = (kr_n - 1)e^{-kr_n}$ is just

$$\Delta F_{1st-order}(h) = \left[\frac{(kr_T + 1)}{2} + \frac{(kr_T)^2}{12} \right] e^{-kr_T} \quad (B6)$$

Whose dependence on h comes by the hand of $r_T(h) = r_{n=1}(h)$. We highlight here such dependence because for most distances $r_T \ll 1$, and $\Delta F_{1st-order}$ is negligible compared to the leading term. The correction term only becomes relevant in the long distances regime, where $A_{ham}^{\omega_n=0}$ provides the dominant contribution of the van der Waals interaction, so we can neglect $\Delta F_{1st-order}$ safely and approximate

$$A_{ham}^{\omega_n>0}(h) \approx \frac{3k_B T}{2} \sum_{k=1}^{\infty} \int_{n=1}^{\infty} R_k(n, x_{1,k}, h) [kr_n + 1] e^{-kr_n} dn \quad (B7)$$

Now we change the variable as $r_n \rightarrow \nu h$, so that $\nu(n) = (4\pi k_B T \epsilon_{med}^{1/2} n) / (c\hbar)$, and we define $\nu_T = \nu(n=1)$. As ϵ_{med} is in general also a function of n , this transformation implies that

$$d\nu = \frac{4\pi k_B T}{c\hbar} \epsilon_{med}^{1/2} dn \left[1 + \frac{1}{2} \frac{d \ln \epsilon_{med}}{d \ln \omega_n} \right] \quad (B8)$$

And we name the term inside the brackets as j_{med} . Plugging this in Eq. B7 and defining $\tilde{R}_k(\nu, x, h) = \epsilon_{med}^{-1/2} j_{med}^{-1} R_k(\nu, x, h)$ leads to

$$A_{ham}^{\omega_n>0}(h) = \frac{3c\hbar}{8\pi} \sum_{k=1}^{\infty} \int_{\nu_T}^{\infty} \tilde{R}_k(\nu, x_{1,k}, h) [k\nu h + 1] e^{-k\nu h} d\nu \quad (B9)$$

The particularization along the same line described above recovers the Eq. 6 of the main text. It is in this stage that we introduce the material parameter ν_{∞} via the inclusion of the factor $e^{\nu/\nu_{\infty}} e^{-\nu/\nu_{\infty}}$ inside the integrand. This allows the evaluation of the integral through a Gaussian Quadrature with the weight function $w(\nu) = e^{-\nu/\nu_{\infty}} [k\nu h + 1] e^{-k\nu h}$, that drops exponentially as ν approaches ν_{∞} . Thus we solve

$$I_0 = \int_{\nu_T}^{\infty} e^{-\nu/\nu_{\infty}} [k\nu h + 1] e^{-k\nu h} d\nu = \quad (B10)$$

$$= \nu_{\infty} \frac{(\nu_T k h + 1)(\nu_{\infty} k h + 1) + \nu_{\infty} k h}{(\nu_{\infty} k h + 1)^2} e^{-\nu_T k h - \frac{\nu_T}{\nu_{\infty}}}$$

$$I_1 = \int_{\nu_T}^{\infty} \nu e^{-\nu/\nu_{\infty}} [k\nu h + 1] e^{-k\nu h} d\nu =$$

$$= \nu_{\infty} \frac{(\nu_T k h + 1)(\nu_{\infty} k h + 1)^2 \nu_T + (2\nu_T k h + 1)(\nu_{\infty} k h + 1) \nu_{\infty} + 2\nu_{\infty}^2 k h}{(\nu_{\infty} k h + 1)^3} e^{-\nu_T k h - \frac{\nu_T}{\nu_{\infty}}}$$

We name the quadrature point $\nu_k^* = I_1/I_0$ to avoid any confusion with ν_T . Besides, we define $\xi_k = (\nu_k^* - \nu_T)/\nu_{\infty}$ for compactness in the formula. The resulting expression is readily particularized to get the Eq. 8 of the main text.

Appendix C: Quadrature for the Hamaker constant

The derivation of the Quadrature expression for the Hamaker constant departs from Eq. B9 in the $h \rightarrow 0$ limit. We further change the variable as $\nu \rightarrow 2\epsilon_{med}^{1/2}\omega/c$, with $\omega_T = \omega_{n=1}$, and introduce again the summation inside the integral, to reach

$$A_{ham}^{\omega_n > 0}(h \rightarrow 0) = \frac{3\hbar}{4\pi} \int_{\omega_T}^{\infty} \sum_{k=1}^{\infty} R_k(\omega, h \rightarrow 0) d\nu \quad (C1)$$

$$R_k(\omega, h \rightarrow 0) = \left[\left(\frac{\epsilon_1 - \epsilon_{med}}{\epsilon_1 + \epsilon_{med}} \right) \left(\frac{\epsilon_2 - \epsilon_{med}}{\epsilon_2 + \epsilon_{med}} \right) \right]^k \frac{1}{k^3}$$

Note that, as explained in the main text, $R_k(\omega, x, h \rightarrow 0)$ no longer depends on x . Also, recall that the dependence on ω enters by the hand of $\epsilon_{i,med} = \epsilon_{i,med}(\omega)$.

The first mean value theorem states that, given the integral of a certain function, $f(x)$, times a probability density function, $w(x)$, there is a certain point, say x^* , such that

$$\int_a^b f(x)w(x)dx = f(x^*) \int_a^b w(x)dx \quad (C2)$$

This generalized form of the first mean value theorem holds as long as $f(x)$ is a continuous real-valued function and $w(x)$ is an integrable nonnegative function. Moreover, realize that if $w(x)$ is the PDF of the continuous uniform distribution, then the usual form of the first mean value theorem is recovered. Also, we define $f(x^*) \equiv f^*$ henceforth.

We apply this version of the first mean value theorem to Eq. C1. We begin developing the integrand up to second order of the summation as

$$\sum_{k=1}^{\infty} R_k(\omega, h \rightarrow 0) = \left(\sum_{k=1}^{\infty} \frac{R_1(\omega)^{k-1}}{k^3} \right) R_1(\omega) \quad (C3)$$

Where $R_1(\omega) = R_{k=1}(\omega)$. We proceed by employing the first mean value theorem with $w(x) \leftrightarrow R_1(\omega)$, and requiring the output to match the exact solution of the original integral up to second order in the expansion. This allows us to write $f^* \leftrightarrow R^*$ in terms of the resulting integrals, and then extend it to the complete series in Eq. C3. This way, the Eq. 12 of the main text is achieved, that is exact up to second order by construction, but approximates very well the rest of the series. The Hamaker constant of the Quadrature is consequently given in terms of the trilogarithm function of R^*

$$Li_3(x) = \sum_{k=1}^{\infty} \frac{x^k}{k^3} \quad (C4)$$

Appendix D: Analytic solution within the Drude model

Here we particularize for the system that we handle by stating that the medium in between the two plates is vacuum, and that both plates are composed of the same metal. Consequently, $\epsilon_{1,2}(\omega) = \epsilon_m$, $\epsilon_{med}(\omega) = \epsilon_v(\omega) = 1.0$, and $j_{med} = j_v = 1.0$. Within the Drude model, $R_{k=1}(\omega, h \rightarrow 0)$ in Eq. C1 becomes

$$R_1(\omega, h \rightarrow 0) = \left(\frac{\omega_P^2}{\omega_P^2 + 2\gamma\omega + 2\omega^2} \right)^2 \quad (D1)$$

Where ω_P and γ are the plasma frequency and the damping coefficient, respectively. As explained in the main text, these are the parameters of the Drude model that characterize the dielectric response of the specific metallic species of the plates. The previous can be further developed approximating that for low ω , $\omega_P^2 \gg 2\gamma\omega$, and for large ω , $2\omega^2 \gg 2\gamma\omega$. Then

$$R_1(\omega, h \rightarrow 0) \approx \left(\frac{\omega_P^2}{\omega_P^2 + 2\omega^2} \right)^2 = \left(\frac{1}{1 + 2(\omega/\omega_P)^2} \right)^2$$

In the following lines, we demonstrate that an analytic expression of ν_∞ for the Drude model can be achieved by requiring the Hamaker constant of the WQA to match the Quadrature of the previous section. First, we take the $h \rightarrow 0$ limit of the WQA in Eq. 8 of the main text.

We write $R_k(\omega, h \rightarrow 0)$ in terms of the preceding result for $k = 1$. In the WQA, this function is evaluated at $(\omega_T + \omega_\infty) = (\nu_T + \nu_\infty)\frac{c}{2}$. Subsequently, we define $f = (\omega_T + \omega_\infty)/\omega_P$ to reach

$$A_{WQA}^{\omega_n > 0}(h \rightarrow 0) \approx \frac{3e\hbar}{4\pi} f \omega_P \sum_{k=1}^{\infty} \frac{1}{k^3} \left(\frac{1}{1 + 2f^2} \right)^{2k} \quad (D2)$$

Where e is the Euler's number and $\omega_\infty \approx f\omega_P$ has been assumed, neglecting ω_T for the sake of simplicity. The next step is to get the corresponding Hamaker constant of the Quadrature based on the first mean value theorem, for what we realize that I_1 and I_2 in Eq. 15 of the main text are analytically solvable for the $R_1(\omega, h \rightarrow 0)$ provided by Eq. D1, namely

$$I_1 = \frac{\omega_P^4}{\Delta} \left[\frac{4\pi}{\Delta^{1/2}} - \frac{g'(\omega_T)}{g(\omega_T)} - \frac{8}{\Delta^{1/2}} \arctan \left(\frac{g'(\omega_T)}{\Delta^{1/2}} \right) \right] \quad (D3)$$

$$I_2 = \frac{\omega_P^8}{3\Delta^3} \left[\frac{480\pi}{\Delta^{1/2}} - \frac{960}{\Delta^{1/2}} \arctan \left(\frac{g'(\omega_T)}{\Delta^{1/2}} \right) - \frac{120g'(\omega_T)}{g(\omega_T)} - \frac{10\Delta g'(\omega_T)}{g^2(\omega_T)} - \frac{\Delta^2 g'(\omega_T)}{g^3(\omega_T)} \right]$$

$$\Delta = 8\omega_P^2 - 4\gamma^2, \quad g(\omega_T) = 2\omega_T^2 + 2\gamma\omega_T + \omega_P^2, \quad g'(\omega_T) = 4\omega_T + 2\gamma$$

These solutions allows us to get the Hamaker constant of the Quadrature exactly, but aimed at providing an analytic formula for ν_∞ , we must approximate $\omega_P^2 \gg \gamma^2$, $\gamma\omega_T$, ω_T^2 . Under this condition, the previous integrals get simplified, and R^* in Eq. 15 of the main text is easily evaluated.

The purpose of the approximations that we have carried out is now unveiled. When we require $A_{WQA}^{\omega_n > 0}(h \rightarrow 0)$ of Eq. D2 to match $A_{ham}^{\omega_n > 0}(h \rightarrow 0)$ of Eq. 17 of the main text, the resulting equality is a transcendental equation for f with a few dimensionless factors

$$f \sum_{k=1}^{\infty} \frac{1}{k^3} \left(\frac{1}{1 + 2f^2} \right)^{2k} = \frac{\sqrt{2}\pi}{5e} Li_3(5/8) \quad (D4)$$

We solve Eq. D4 numerically to get two possible solutions. Either $f_1 = 0.250141$ or $f_2 = 0.553656$ fulfill the condition imposed by Eq. D4. This happens because $\nu_\infty R_k(\nu_T + \nu_\infty)$ is a non-monotonic function of ν_∞ , but only the ν_∞ that emerges from f_2 preserves the desired habit of $A_{ham}^{\omega_n > 0}(h)$.

Finally, we return to the definition of f to achieve

$$\omega_\infty = f\omega_P - \omega_T \quad (D5)$$

With $f = 0.553656$, which is the Eq. 18 of the main text. The accuracy of the approximations performed is verified in Fig. 1 of the main text.